Conference Paper, Published Version

Onda, Shinichiro; Hosoda, Takashi; Kimura, Ichiro

Refinement of a Depth Averaged Flow Model in Curved Channel in Generalized Curvilinear Coordinate System

REFINEMENT OF A DEPTH AVERAGED FLOW MODEL IN CURVED CHANNEL IN GENERALIZED CURVILINEAR COORDINATE SYSTEM

Shinichiro Onda [1], Takashi Hosoda [2] and Ichiro Kimura [3]

[1] Assistant Professor, Department of Urban Management, Kyoto University
Kyoto-Daigaku-Katsura, Nishikyo-ku, Kyoto, 615-8540, Japan, e-mail: sonda@mbox.kudpc.kyoto-u.ac.jp
[2] Professor, Department of Urban Management, Kyoto University
Kyoto-Daigaku-Katsura, Nishikyo-ku, Kyoto, 615-8540, Japan, e-mail: hosoda@mbox.kudpc.kyoto-u.ac.jp
[3] Associate Professor, Faculty and Graduate School of Engineering, Hokkaido University
Nishi-8, Kita-13, Kita-ku, Sapporo, 060-8623, Japan, e-mail: i-kimu2@eng.hokudai.ac.jp

ABSTRACT

In curved channels, velocity distribution in the main flow direction is transformed by the secondary currents and the strength of secondary circulation is varied with the deformation of longitudinal velocity. Therefore, in order to predict such flows more accurately, it is necessary to include the effects caused by the interaction between main and secondary flows. In this study, a refinement of depth averaged flow model for the curved channels in generalized curvilinear coordinate system is examined by considering this interaction. The refined model is applied to simulate the flows of previous laboratory experiments for a uniformly curved channel conducted by Rozovskii (1961). The calculated results are compared with the experimental and 3D numerical results to verify the fundamental characteristics of this model.

Keywords: depth averaged flow model, curved channel, secondary currents and generalized curvilinear coordinate system

1. INTRODUCTION

A depth averaged flow model in generalized curvilinear coordinate system is commonly used to simulate flows in rivers. In some cases, 3D model is also applied to some parts of river sections, where the secondary currents are generated; and in these cases the depth averaged model cannot simulate the flow correctly. However, the application of 3D model is difficult and time consuming. In such sections, in order to apply depth averaged flow model, the effects of secondary circulation are necessary to be included to evaluate the momentum transport and bottom shear stress correctly.

A number of attempts have been made to study and develop the model for secondary currents and include the effects of secondary flow into a depth averaged flow model. Ishikawa and Kim (1986) conducted the hydraulic experiments for the flow in a uniformly curved channel, and pointed out that interaction between the main and secondary flows affects the strength of secondary circulation. Blanckaert (2002) carried out the experiments for sharply curved channels and he observed the transformation of velocity distribution in the main flow direction due to the secondary currents. He pointed out that the linear model, in which the velocity distribution in streamwise direction is assumed to be uniform, overestimates the momentum transport. Furthermore, he compared the order of each terms in a momentum equation from the experimental results and examined the effective terms for the transformation of streamwise velocity.

On the other hand, Ikeda and Nishimura (1986) and Johannesson and Parker (1989) pointed out that it is necessary to consider the development and attenuation of secondary currents (the lag between the curvature of stream line and secondary currents). Hosoda et al. (2001) developed the depth averaged flow model in generalized curvilinear coordinate system including the development and attenuation of secondary currents. But, to evaluate the momentum transport, they applied the model proposed by Engelund (1974), in which the velocity distribution in main flow direction is assumed to be uniform.

Though some models are proposed which consider the interaction between the main and secondary flows, the redistribution modeling of velocity distribution in streamwise direction due to secondary currents is not incorporated into the depth averaged flow model.

In this study, a depth averaged flow model for curved channels is refined by including the deformation of main flow velocity distribution due to secondary currents and introducing the development and attenuation of secondary currents. The refined model is applied to simulate the flows of previous laboratory experiments for a uniformly curved channel conducted by Rozovskii (1961). The calculated results are compared with the experimental and 3D numerical results.

2. DEPTH AVERAGED FLOW MODEL

2.1 Basic equations

A depth averaged flow model with the effect of transverse momentum transport due to secondary currents is described as follows (Hosoda et al., 2001):

[Continuity equation]

$$\frac{\partial}{\partial t}\left(\frac{h}{J}\right)+\frac{\partial}{\partial \xi}\left(\frac{Uh}{J}\right)+\frac{\partial}{\partial \eta}\left(\frac{Vh}{J}\right)=0 \tag{1}$$

[Momentum equation]

$$\begin{aligned}
&\frac{\partial}{\partial t}\left(\frac{Q^{\xi}}{J}\right)+\frac{\partial}{\partial \xi}\left(\frac{UQ^{\xi}}{J}\right)+\frac{\partial}{\partial \eta}\left(\frac{VQ^{\xi}}{J}\right)-\frac{M}{J}\left(U\frac{\partial \xi_x}{\partial \xi}+V\frac{\partial \xi_x}{\partial \eta}\right)-\frac{N}{J}\left(U\frac{\partial \xi_y}{\partial \xi}+V\frac{\partial \xi_y}{\partial \eta}\right)\\
&\quad=-Gh\left(\frac{\xi_x^2+\xi_y^2}{J}\frac{\partial z_s}{\partial \xi}+\frac{\xi_x\eta_x+\xi_y\eta_y}{J}\frac{\partial z_s}{\partial \eta}\right)-\frac{\tau_b^{\xi}}{\rho J}+\frac{\xi_x^2}{J}\frac{\partial}{\partial \xi}\left(-\overline{u'^2}h\right)+\frac{\xi_x\eta_x}{J}\frac{\partial}{\partial \eta}\left(-\overline{u'^2}h\right)\\
&\quad+\frac{\xi_y^2}{J}\frac{\partial}{\partial \xi}\left(-\overline{v'^2}h\right)+\frac{\xi_y\eta_y}{J}\frac{\partial}{\partial \eta}\left(-\overline{v'^2}h\right)+\frac{2\xi_x\xi_y}{J}\frac{\partial}{\partial \xi}\left(-\overline{u'v'}h\right)+\frac{\xi_x\eta_y+\xi_y\eta_x}{J}\frac{\partial}{\partial \eta}\left(-\overline{u'v'}h\right)\\
&\quad-\xi_x\left(S_{\xi 1}+S_{\xi 2}+S_{\xi 3}+S_{\xi 4}\right)-\xi_y\left(S_{\eta 1}+S_{\eta 2}+S_{\eta 3}+S_{\eta 4}\right)
\end{aligned} \tag{2a}$$

$$\begin{aligned}
&\frac{\partial}{\partial t}\left(\frac{Q^{\eta}}{J}\right)+\frac{\partial}{\partial \xi}\left(\frac{UQ^{\eta}}{J}\right)+\frac{\partial}{\partial \eta}\left(\frac{VQ^{\eta}}{J}\right)-\frac{M}{J}\left(U\frac{\partial \eta_x}{\partial \xi}+V\frac{\partial \eta_x}{\partial \eta}\right)-\frac{N}{J}\left(U\frac{\partial \eta_y}{\partial \xi}+V\frac{\partial \eta_y}{\partial \eta}\right)\\
&\quad=-Gh\left(\frac{\xi_x\eta_x+\xi_y\eta_y}{J}\frac{\partial z_s}{\partial \xi}+\frac{\eta_x^2+\eta_y^2}{J}\frac{\partial z_s}{\partial \eta}\right)-\frac{\tau_b^{\eta}}{\rho J}+\frac{\xi_x\eta_x}{J}\frac{\partial}{\partial \xi}\left(-\overline{u'^2}h\right)+\frac{\eta_x^2}{J}\frac{\partial}{\partial \eta}\left(-\overline{u'^2}h\right)\\
&\quad+\frac{\xi_y\eta_y}{J}\frac{\partial}{\partial \xi}\left(-\overline{v'^2}h\right)+\frac{\eta_y^2}{J}\frac{\partial}{\partial \eta}\left(-\overline{v'^2}h\right)+\frac{\xi_x\eta_y+\xi_y\eta_x}{J}\frac{\partial}{\partial \xi}\left(-\overline{u'v'}h\right)+\frac{2\eta_x\eta_y}{J}\frac{\partial}{\partial \eta}\left(-\overline{u'v'}h\right)\\
&\quad-\eta_x\left(S_{\xi 1}+S_{\xi 2}+S_{\xi 3}+S_{\xi 4}\right)-\eta_y\left(S_{\eta 1}+S_{\eta 2}+S_{\eta 3}+S_{\eta 4}\right)
\end{aligned} \tag{2b}$$

where t = time; ξ, η = generalized curvilinear coordinates; J = Jacobian of coordinate transformation; Q^{ξ}, Q^{η} = contravariant components of discharge flux vectors for unit width; M, N = Cartesian components of discharge flux vectors; U, V = contravariant components of velocity vectors; h = depth; z_s = water surface elevation from datum plane; G = gravitational acceleration; τ_b^{ξ}, τ_b^{η} = contravariant components of bottom shear stress vectors; $-\overline{u'^2}, -\overline{u'v'}, -\overline{v'^2}$ = Cartesian components of Reynolds stress tensors. $S^{\xi}{}_1$-$S^{\eta}{}_4$ are additional terms which include the effects of secondary currents defined as follows.

$$S_{\xi 1} = -c_{sn} \frac{\partial}{\partial \xi}\left[\frac{1}{J}\left(\xi_x A_n \bar{u}_s h \sin 2\varphi - \xi_y A_n \bar{u}_s h \cos 2\varphi\right)\right] \tag{3a}$$

$$S_{\xi 2} = -c_{sn} \frac{\partial}{\partial \eta}\left[\frac{1}{J}\left(\eta_x A_n \bar{u}_s h \sin 2\varphi - \eta_y A_n \bar{u}_s h \cos 2\varphi\right)\right] \tag{3b}$$

$$S_{\xi 3} = c_{n2} \frac{\partial}{\partial \xi}\left[\frac{1}{J}\left(\xi_x A_n^2 h \sin^2 \varphi - \xi_y A_n^2 h \cos\varphi \sin\varphi\right)\right] \tag{3c}$$

$$S_{\xi 4} = c_{n2} \frac{\partial}{\partial \eta}\left[\frac{1}{J}\left(\eta_x A_n^2 h \sin^2 \varphi - \eta_y A_n^2 h \cos\varphi \sin\varphi\right)\right] \tag{3d}$$

$$S_{\eta 1} = c_{sn} \frac{\partial}{\partial \xi}\left[\frac{1}{J}\left(\xi_x A_n \bar{u}_s h \cos 2\varphi + \xi_y A_n \bar{u}_s h \sin 2\varphi\right)\right] \tag{3e}$$

$$S_{\eta 2} = c_{sn} \frac{\partial}{\partial \eta}\left[\frac{1}{J}\left(\eta_x A_n \bar{u}_s h \cos 2\varphi + \eta_y A_n \bar{u}_s h \sin 2\varphi\right)\right] \tag{3f}$$

$$S_{\eta 3} = -c_{n2} \frac{\partial}{\partial \xi}\left[\frac{1}{J}\left(\xi_x A_n^2 h \sin\varphi \cos\varphi - \xi_y A_n^2 h \cos^2 \varphi\right)\right] \tag{3g}$$

$$S_{\eta 4} = -c_{n2} \frac{\partial}{\partial \eta}\left[\frac{1}{J}\left(\eta_x A_n^2 h \cos\varphi \sin\varphi - \eta_y A_n^2 h \cos^2 \varphi\right)\right] \tag{3h}$$

where $\bar{u}_s$ = depth averaged velocity in s-direction; A_n = representative velocity of secondary currents; s = spatial coordinate along the stream line, n = spatial coordinate perpendicular to s and z coordinates; c_{sn} and c_{n2} = momentum transport coefficients; φ = angle between a stream line and x-axis. We assume that the velocity distributions in s and n directions can be expressed by Equation (4), and then the momentum transport coefficients c_{sn} and c_{n2} are defined in Equation (5).

$$u_s = \bar{u}_s \cdot f_s(\zeta), \quad u_n = A_n \cdot f_n(\zeta) \tag{4}$$

$$c_{s2} = \int_0^1 f_s(\zeta)^2 d\zeta, \quad c_{sn} = \int_0^1 f_s(\zeta) f_n(\zeta) d\zeta, \quad c_{n2} = \int_0^1 f_n(\zeta)^2 d\zeta \tag{5}$$

where $f_s(\zeta)$ and $f_n(\zeta)$ = similarity functions of velocity distribution. In this case, c_{s2} is assumed to be 1.

In previous studies (Ikeda and Nishimura, 1986; Johannesson and Parker, 1989), it was shown that it is necessary to include the lag between the curvature of stream line and the secondary currents. The development and attenuation process of secondary currents can be described by the following approximate expression of vorticities (Muramoto and Inoue, 1965; Hosoda et al., 2001).

$$\begin{aligned} &\frac{\partial}{\partial t}\left\{\frac{(u_n)_s - (u_n)_b}{J}\right\} + \frac{\partial}{\partial \xi}\left\{\frac{U_s}{J}(u_n)_s - \frac{U_b}{J}(u_n)_b\right\} + \frac{\partial}{\partial \eta}\left\{\frac{V_s}{J}(u_n)_s - \frac{V_b}{J}(u_n)_b\right\} - \frac{1}{Jr}\left\{(u_s^2)_s - (u_s^2)_b\right\} \\ &\quad = \frac{1}{J}\frac{\partial}{\partial z}\left(\frac{\tau_{zn}}{\rho}\right)_s - \frac{1}{J}\frac{\partial}{\partial z}\left(\frac{\tau_{zn}}{\rho}\right)_b \\ &\quad + \alpha h u_* \lambda \left\{\frac{\xi_x^2 + \xi_y^2}{J}\frac{\partial^2 A_n}{\partial \xi^2} + \frac{\xi_x \eta_x + \xi_y \eta_y}{J}\frac{\partial^2 A_n}{\partial \eta^2}\right\} + \alpha h u_* \lambda \left\{\frac{\xi_x \eta_x + \xi_y \eta_y}{J}\frac{\partial^2 A_n}{\partial \xi^2} + \frac{\eta_x^2 + \eta_y^2}{J}\frac{\partial^2 A_n}{\partial \eta^2}\right\} \end{aligned} \tag{6}$$

where r = radius of curvature of a stream line. Subscripts s and b denote the variables at surface and bottom, respectively, and α is equal to 0.5.

The term $(u_n)_s$–$(u_n)_b$ in the left hand side of Equation (6) is related to A_n, in which the effects of lag between the curvature of stream line and secondary currents is also included.

$$(u_n)_s - (u_n)_b = \lambda \cdot A_n \tag{7}$$

2.2 Modeling of velocity distribution considering the interaction between the main and secondary flows

In order to evaluate the momentum transport coefficients and some terms in Equation (6), it is necessary to derive the velocity distributions. Hosoda et al. (2001) applied the model by Engelund (1974) (Equation (8)) to obtain the velocity distribution in *s*-direction.

$$G\sin\theta+\frac{\partial}{\partial z}\left(\varepsilon_e\frac{\partial u_s}{\partial z}\right)=0 \tag{8}$$

where θ = bed slope; ε_e = eddy viscosity coefficient (= $\beta h u_*$, β = 0.077).

On the other hand, based on the experimental results, Blanckaert (2002) pointed out that the advection terms $-(u_n\partial u_s/\partial n+u_s u_n/r)$ play an important role in redistribution of u_s. Furthermore, he assumed that the velocity distribution u_s can be described as a power-law function of *n*. He used the following relation for transverse gradient of downstream velocity to derive the velocity distribution in streamwise direction.

$$\partial u_s/\partial n=\alpha_s\, u_s/r \tag{9}$$

In this study, we apply the mathematical model proposed by Engelund (1974) and Blankaert (2002) and introduce the advection term $-u_s u_n/r$ into Equation (8). This physical mechanism is described as follows: in curved channels, the flow direction at surface is outward, while at bottom layer it is inward due to secondary currents. Thus, u_s and r are positive in both layers, while u_n is positive at surface and negative in bottom. So, the term $-u_s u_n/r$ becomes negative and positive in those two layers, respectively. Therefore, this term tends to decelerate the streamwise velocity in the surface layer and accelerate it in the bottom layer. The momentum equations in *s* and *n* directions can be described as follows.

[Momentum equation in *s*-direction]

$$-\frac{u_s u_n}{r}+G\sin\theta+\frac{\partial}{\partial z}\left(\varepsilon_e\frac{\partial u_s}{\partial z}\right)=0 \tag{10a}$$

[Momentum equation in *n*-direction]

$$\frac{u_s^{\,2}}{r}+\varepsilon_e\frac{\partial^2 u_n}{\partial z^2}-G\frac{\partial h}{\partial r}=0 \tag{10b}$$

The procedure for deriving the velocity distribution from Equation (10) is described as follows with assumption that the velocity distributions in *s* and *n* directions are expressed by the power-law.

$$\frac{u_s}{\bar{u}_s}=C_0+C_1\zeta+C_2\zeta^2+C_3\zeta^3+C_4\zeta^4+C_5\zeta^5+C_6\zeta^6+C_7\zeta^7 \tag{11a}$$

$$\frac{u_n}{\bar{u}_s}=D_0+D_1\zeta+D_2\zeta^2+D_3\zeta^3+D_4\zeta^4+D_5\zeta^5+D_6\zeta^6+D_7\zeta^7 \tag{11b}$$

Substituting Equations (11) into Equations (10) and integrating Equations (10) in the depth direction, the coefficients C_i and D_i are obtained.

$$C_0=\frac{u_{sb}}{\bar{u}_s}=\frac{r_* u_*}{\bar{u}_s} \tag{12a}$$

$$\begin{aligned}C_1=\frac{C_0}{\beta r_*}-\delta\Big[&C_0D_0+\frac{1}{2}(C_0D_1+C_1D_0)+\frac{1}{3}(C_0D_2+C_1D_1+C_2D_0)\\&+\frac{1}{4}(C_0D_3+C_1D_2+C_2D_1+C_3D_0)+\frac{1}{5}(C_0D_4+C_1D_3+C_2D_2+C_3D_1+C_4D_0)\\&+\frac{1}{6}(C_0D_5+C_1D_4+C_2D_3+C_3D_2+C_4D_1+C_5D_0)\\&+\frac{1}{7}(C_0D_6+C_1D_5+C_2D_4+C_3D_3+C_4D_2+C_5D_1+C_6D_0)\end{aligned} \tag{12b}$$

$$+\frac{1}{8}\left(C_0D_7+C_1D_6+C_2D_5+C_3D_4+C_4D_3+C_5D_2+C_6D_1+C_7D_0\right)\Big]$$

$$C_2=-\frac{1}{2}\frac{C_0}{\beta r_*}+\frac{1}{2}\delta C_0D_0 \tag{12c}$$

$$C_3=\frac{1}{6}\delta\left(C_0D_1+C_1D_0\right) \tag{12d}$$

$$C_4=\frac{1}{12}\delta\left(C_0D_2+C_1D_1+C_2D_0\right) \tag{12e}$$

$$C_5=\frac{1}{20}\delta\left(C_0D_3+C_1D_2+C_2D_1+C_3D_0\right) \tag{12f}$$

$$C_6=\frac{1}{30}\delta\left(C_0D_4+C_1D_3+C_2D_2+C_3D_1+C_4D_0\right) \tag{12g}$$

$$C_7=\frac{1}{42}\delta\left(C_0D_5+C_1D_4+C_2D_3+C_3D_2+C_4D_1+C_5D_0\right) \tag{12h}$$

$$D_0=\frac{u_{nb}}{\bar{u}_s} \tag{13a}$$

$$D_1=\frac{D_0}{\beta r_*} \tag{13b}$$

$$\begin{aligned}D_2=\frac{1}{2}\delta\Big[&C_0C_1+\frac{2}{3}C_0C_2+\frac{1}{3}C_1^2+\frac{1}{2}C_0C_3+\frac{1}{2}C_1C_2+\frac{2}{5}C_0C_4+\frac{2}{5}C_1C_3+\frac{1}{5}C_2^2\\&+\frac{1}{3}C_0C_5+\frac{1}{3}C_1C_4+\frac{1}{3}C_2C_3+\frac{2}{7}C_0C_6+\frac{2}{7}C_1C_5+\frac{2}{7}C_2C_4\\&+\frac{1}{7}C_3^2+\frac{1}{4}C_0C_7+\frac{1}{4}C_1C_6+\frac{1}{4}C_2C_5+\frac{1}{4}C_3C_4\Big]-\frac{1}{2}\frac{D_0}{\beta r_*}\end{aligned} \tag{13c}$$

$$D_3=-\frac{1}{3}\delta C_0C_1 \tag{13d}$$

$$D_4=-\frac{1}{12}\delta\left(2C_0C_2+C_1^2\right) \tag{13e}$$

$$D_5=-\frac{1}{10}\delta\left(C_0C_3+C_1C_2\right) \tag{13f}$$

$$D_6=-\frac{1}{30}\delta\left(2C_0C_4+2C_1C_3+C_2^2\right) \tag{13g}$$

$$D_7=-\frac{1}{21}\delta\left(C_0C_5+C_1C_4+C_2C_3\right) \tag{13h}$$

where $\delta = h\bar{u}_s/(\beta u_* r)$.

In addition, the following expressions for coefficients C_i and D_i are obtained by satisfying Equation (14).

$$\bar{u}_s=\frac{1}{h}\int_{z_b}^{z_s}u_s dz\,,\quad \int_{z_b}^{z_s}u_n dz=0 \tag{14}$$

$$C_0+\frac{1}{2}C_1+\frac{1}{3}C_2+\frac{1}{4}C_3+\frac{1}{5}C_4+\frac{1}{6}C_5+\frac{1}{7}C_6+\frac{1}{8}C_7=1 \tag{15a}$$

$$D_0+\frac{1}{2}D_1+\frac{1}{3}D_2+\frac{1}{4}D_3+\frac{1}{5}D_4+\frac{1}{6}D_5+\frac{1}{7}D_6+\frac{1}{8}D_7=0 \tag{15b}$$

The procedure to obtain the coefficients C_i and D_i is described as follows. Firstly, δ and r_* in Equations (12) and (13) are assumed to be known. Then,

1) C_0, C_1 and C_2 are derived by substituting $\delta = 0$ into Equations (12a), (12b) and (12c).
2) C_0, C_1 and C_2 obtained in 1) and δ are substituted in Equations (13). The coefficients D_0-D_7 are obtained to satisfy the Equation (15b).

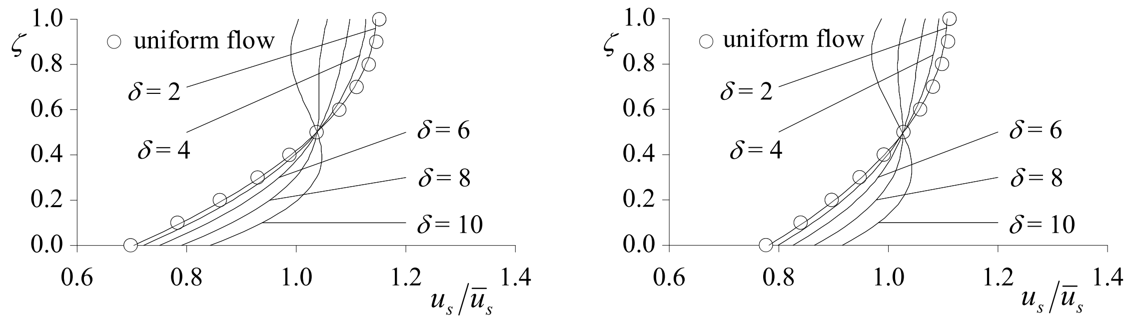

Figure 1 Velocity distribution in streamwise direction (left: r_* = 10, right: r_* = 15)

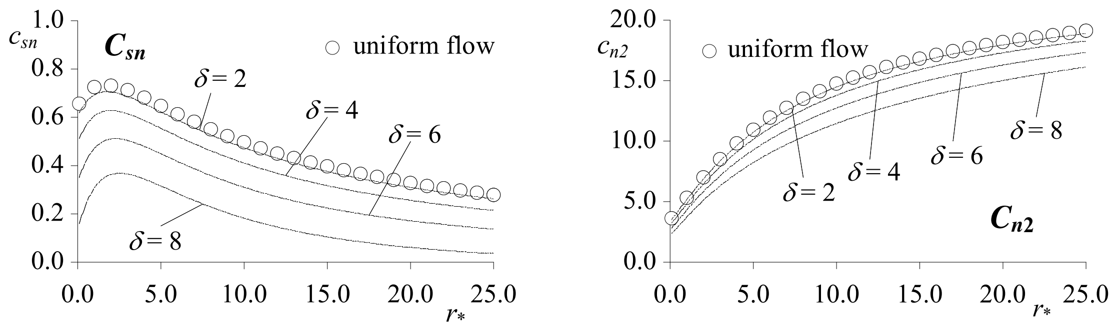

Figure 2 Momentum transport coefficients

3) Substituting D_0-D_7 and δ into Equations (12), C_2-C_7 are derived.
4) To satisfy Equation (15a) and the following relation, C_0 and C_1 are derived.

$$\varepsilon_e \, \partial u_s / \partial z \big|_{z=0} = u_*^2 \tag{16}$$

Note that, the velocity distribution obtained in process 1) and 2) is the same as the Engelund model.

2.3 Fundamental property of velocity distribution and momentum transport coefficients

Here, we examine the fundamental property of velocity distribution and momentum transport coefficients in this model. Figures 1 and 2 show the velocity distributions in the main flow direction and the momentum transport coefficients c_{sn} and c_{n2}, respectively. It can be observed that the velocity distribution is transformed due to the effects of secondary flow in case of large δ, while it coincides with the velocity distribution in uniform flow (Engelund model) in case of small δ. For large δ, the momentum transport coefficients are smaller in comparison to small δ. This is based on the fact that for larger δ, the effects of secondary currents become weak due to the deformation of velocity distribution in streamwise direction. This agrees with the results by Blankaert (2002), and reveals that the linear model, in which the velocity distribution in stream direction is assumed to be uniform, overestimates the momentum transport in curved channel flows.

3. MODEL VERIFICATION

The refined model is applied to simulate the flow of experiments conducted by Rozovskii (1961) for a uniformly curved channel. The hydraulic conditions are presented in Figure 3. No.1 and 2 are the sections at 36^o and 120^o, respectively, from the entrance of curved channel. No. 3 and 4 are located at 0.1m and 0.5m, respectively, downstream of the

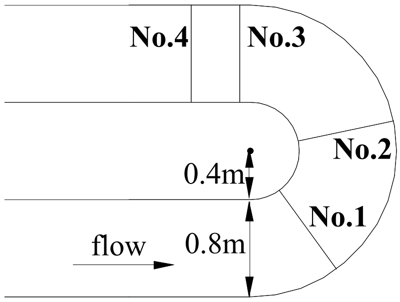

Discharge Q: 12.3l/s, Average depth h: 0.06m, Bed slope: 0

Figure 3 Experimental setup by Rozovskii

exit of curved channel.

For the numerical simulation of refined model, the finite volume method is used and QUICK scheme is applied for the convection terms. The momentum transport coefficients c_{sn} and c_{n2} are multiplied by the dumping function to consider the attenuation of secondary currents strength near the walls.

$$f_w = 1.0 - \left(1.0 - \frac{l}{aB}\right)^2 \tag{17}$$

where l = distance from side wall; B = channel width and a = 0.3.

We tested the following 3 cases namely Run A, Run B and Run C.

[Run A] The effects induced by secondary currents are not included. (Equations (1) and (2) without $S_{\xi 1}$-$S_{\eta 4}$)

[Run B] The effects of secondary currents are included, and Engelund model is used for the velocity distribution.

[Run C] The effects of secondary currents are included, and the model proposed in this study is used for the velocity distribution.

In Run C, the velocity distribution is derived by using the value of δ at each grid point, and the momentum transport coefficients c_{sn} and c_{n2} are calculated. The effects of δ is decreased by multiplying the coefficients by δ, since the velocity distribution in main flow direction deforms much due to large δ and the numerical simulation becomes unstable.

We also conducted a 3D simulation using the Reynolds averaged 3D flow equations with contravariant components of velocity vectors in a moving generalized curvilinear coordinate system. A 2nd-order non-linear k-ε model by Kimura and Hosoda (2003) is adopted as a turbulence model. This model has been applied to various flow fields, such as flows around submerged spur dikes (Kimura et al., 2004).

4. RESULTS AND DISCUSSIONS

Figure 4 and 5 show the water surface elevation and depth averaged velocity distribution in transversal direction. The calculated results obtained for the water surface elevation and depth averaged velocity distribution from Run A, B and C are almost the same at sections No.1 and No.2. Here, only the results for Run C are presented. It is observed that both results obtained from the refined model (Run C) and the 3D model on transversal distribution of water surface elevation are in good agreement with the experiments. It is also seen that the refined model reproduces the experimental results on the distribution of depth averaged velocity at sections No.1 and No.2. On the other hand, at sections No.3 and No.4, which are located at 0.1m and 0.5m downstream of the exit of curved channel, the difference between Run B and Run C can be observed near the inner bank. It is observed that the results

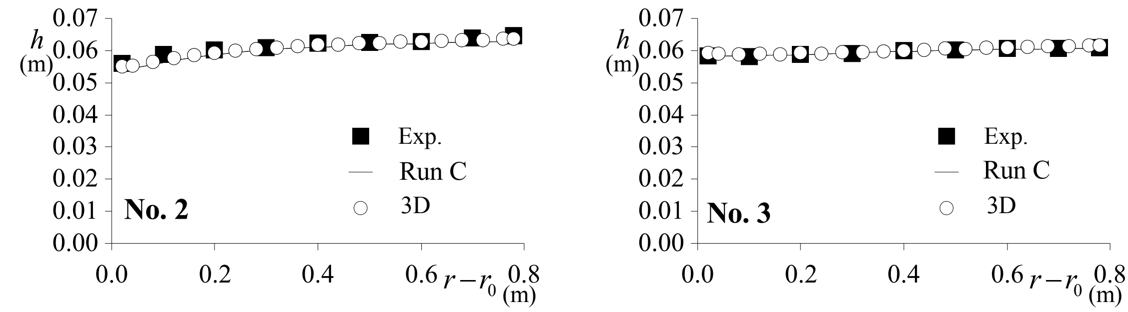

Figure 4 Transversal water level distribution

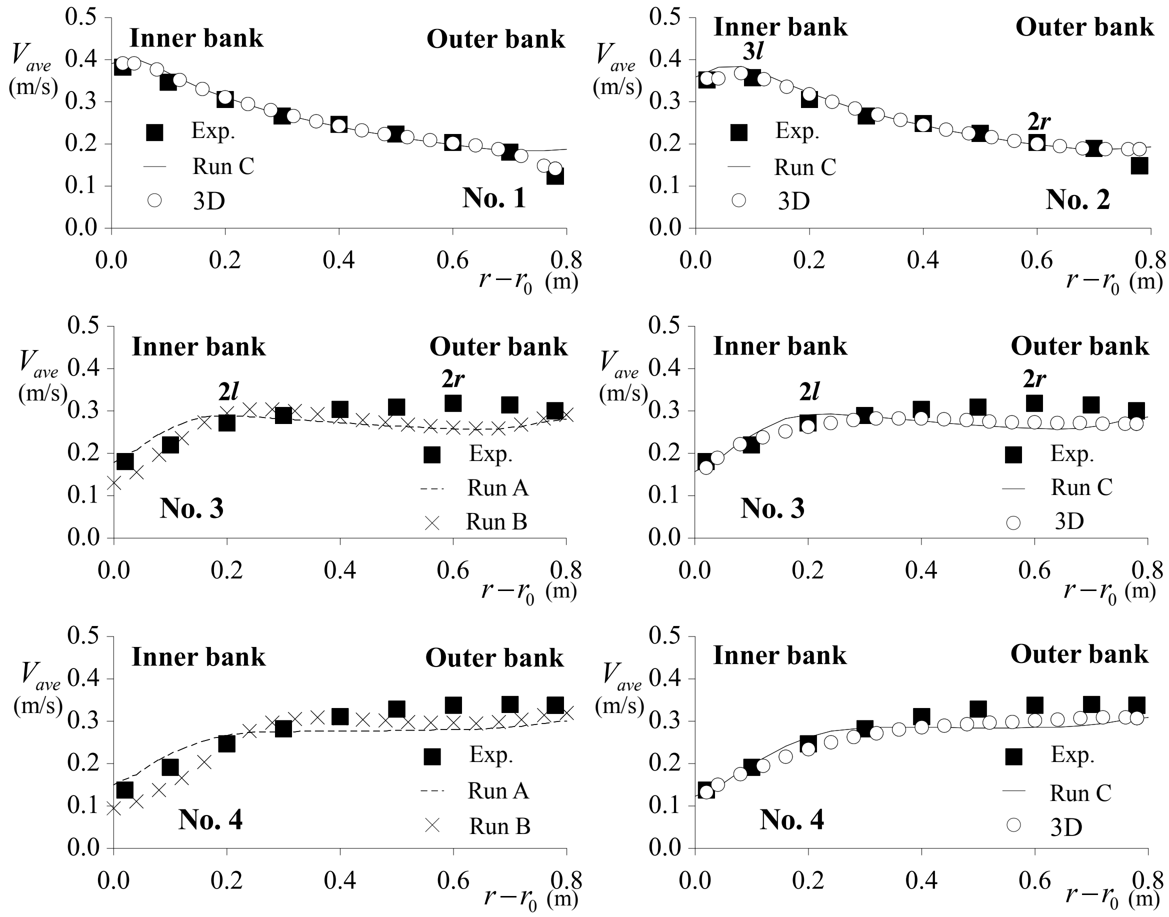

Figure 5 Depth averaged velocity distribution in transversal direction

of the model in Run B are in better agreement than Run A, due to inclusion of the effects of secondary currents. However, the momentum transport is overestimated in Run B, so the velocity gradient is higher. In the results of refined model in Run C, the momentum transport is decreased in comparison with Run B, and the results in Run C agree with the experiments. At the outer bank, the water surface elevation is decreased from the curved to straight channels, and the increment of the depth averaged velocity is observed. So, the calculated results are in close agreement with experimental results. In this case, the results of 3D model are in good agreement with the experiments.

Figure 6 and 7 show the vertical velocity distribution at sections No.3 and No.4 at some points. The deformation of velocity distribution in streamwise direction can be observed in Run C, though the velocity dip is not reproduced. It is thought that the velocity dip can be reproduced by increasing the coefficients, which are multiplied by the value of δ. The strength

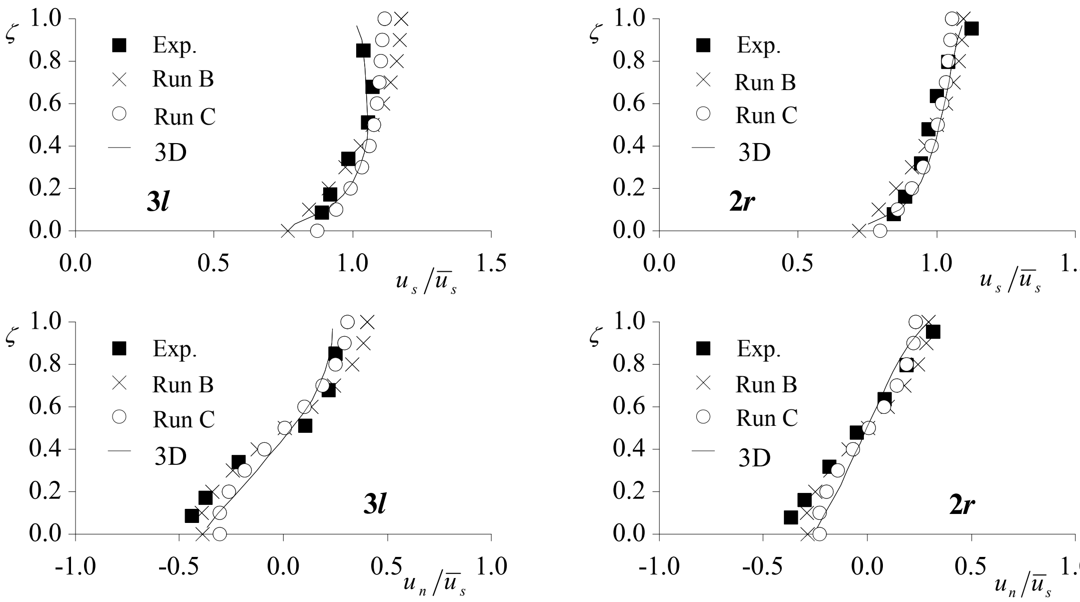

Figure 6 Comparison of velocity distribution at No.2 section
(top: in streamwise direction, bottom: in transversal direction)

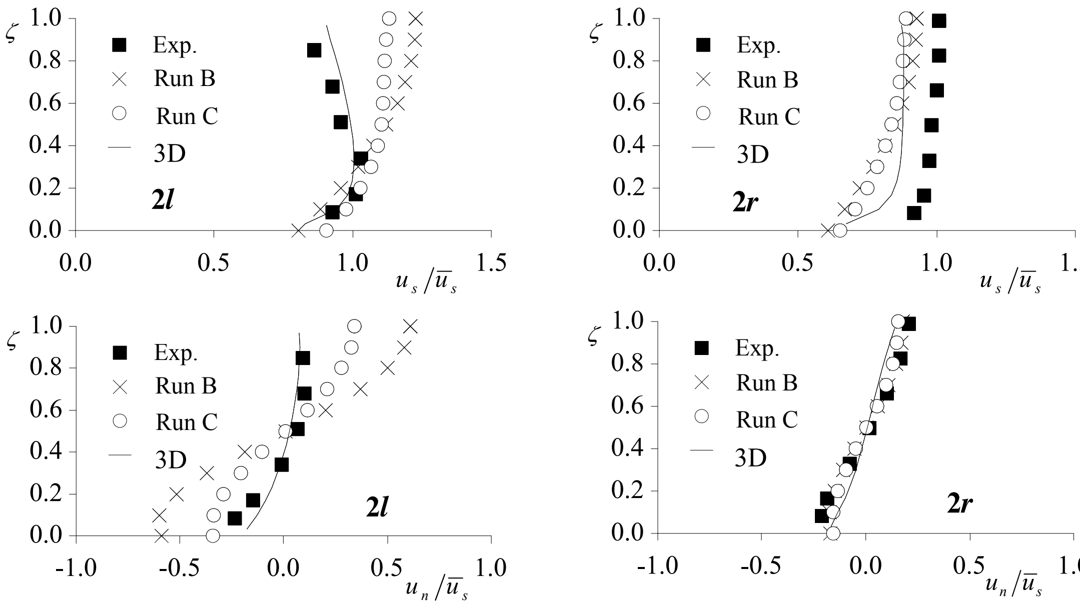

Figure 7 Comparison of velocity distribution at No.3 section
(top: in streamwise direction, bottom: in transversal direction)

of secondary currents is decreased due to this deformation in Run C and the results agree with the experimental results better than in Run B. It should be noted that, in this case, the 3D model can also reproduce the experiments.

5. CONCLUSIONS

In this paper, a depth averaged flow model for a curved channel in generalized curvilinear coordinate system is refined by including the model for deformation of velocity distribution in streamwise direction due to the secondary currents. Based on the results obtained here, it can be concluded that the refined model is capable of simulating flow in curved channel.

REFERENCES

Blanckaert, K. (2002), Flow and turbulence in sharp open-channel bends, PhD-thesis, Ecole Polytechnique Federale de Lausanne.

Blanckaert, K., Glasson, L., Jagers, H.R.A. and Sloff, C.J. (2003), Quasi-3D simulation of flow in sharp open-channel bends with horizontal and developed bed topography, *Proceedings of the International Symposium on Shallow Flows*, Part I, pp.93-100.

Engelund, F. (1974), Flow and bed topography in channel bends, *Proceeding of ASCE*, 100, HY11, pp.1631-1648.

Hosoda, T., Nagata, N., Kimura, I., Michibata, K. and Iwata, M. (2001), A depth averaged model of open channel flows with lag between main flows and secondary currents in a generalized curvilinear coordinate system, *Advances in Fluid Modeling & Turbulence Measurements*, pp.63-70, World Scientific.

Ikeda, S. and Nishimura, T. (1986), Three-dimensional flow and bed topography in sand-silt meandering rivers, *Journal of Hydraulic, Coastal and Environmental Engineering*, 369/II-5, pp.99-108 (in Japanese).

Ishikawa, T. and Kim, S. (1986), A basic study on the development of secondary circulation in curved channels, *Journal of Hydraulic, Coastal and Environmental Engineering*, 375/II-6, pp.143-149 (in Japanese).

Johannesson, H. and Parker, G. (1989), Secondary flow in mildly sinuous channel, *Journal of Hydraulic Engineering*, ASCE, 115(3), pp.289-308.

Kalkwijk, J. P. and De Vriend, H. J. (1980), Computation of the flow in shallow river bends, *Journal of Hydraulic Research*, IAHR, 18(4), pp.327-342.

Kimura, I. and Hosoda, T. (2003), A non-linear k-ε model with realizability for prediction of flows around bluff bodies, *International Journal for Numerical Methods in Fluids*, 42, pp. 813-837, Wiley.

Kimura, I., Hosoda, T., Onda, S. and Tominaga, A. (2004) Computations of 3D turbulent flow structures around submerged spur dikes under various hydraulic conditions, *River Flow 2004*, 1, pp.543-553, Balkema.

Muramoto, Y. and Inoue, T. (1965), Internal structure of flow through curved open channels, *Disaster Prevention Research Institute Annuals*, 8, pp.415-427 (in Japanese).

Rozovskii, I. L. (1961), Flow of water in bends of open channels, *Israel Program for Scientific Translations*, Jerusalem, Israel.